Non-Adiabatic Semiclassical Calculations of the Collision-Time Asymmetry of the ^{114}Cd 326.1 nm Line Perturbed by Noble Gases

A. Bielski, R. Ciuryło, D. Lisak, R.S. Trawiński and T. Orlikowski

Institute of Physics, Nicolaus Copernicus University
Grudziądzka 5/7, 87-100 Toruń, Poland

(Received August 11, 2003; revised version December 15, 2003)

The collision-time asymmetry coefficients as well as the pressure broadening and shifting rates of the ^{114}Cd 326.1 nm line perturbed by noble gases are calculated in the framework of the non-adiabatic semi-classical method using the Czuchaj et al. potentials. The theoretical values are compared with experimental results determined recently by means of laser-induced fluorescence technique.

PACS numbers: 32.70.–n, 33.70.–w, 34.20.–b

1. Introduction

At low densities of perturbing atoms, the core and near wings of collisionally broadened and shifted isolated spectral line can be described by a Lorentzian profile [1, 2]. Such a line profile is justified only in the so-called impact approximation in which the duration of each collision is assumed negligibly short compared with the time between collisions. More detailed theoretical treatment showed, however, that the inclusion of the finite duration of collisions modifies the Lorentzian profile, the first-order correction being the addition of a dispersion component to the Lorentzian distribution. Thus the resulting line shape becomes asymmetric and this type of asymmetry is usually referred to as collision-time asymmetry [3–13].

Spectral line shapes are also determined by thermal motion of the emitting (or absorbing) atom which alters the shape of the line through the Doppler effect,

but it also determines the relative emitter–perturber velocity distribution, and through that the collisional broadening. This means that in general case these effects are not statistically independent and in the line shape analysis we should, in principle, take into account a correlation between the Doppler and collisional broadening, keeping in mind that the collision parameters of the line profiles such as their Lorentzian width and shift are dependent on the emitter velocity.

Berman [14] and Ward et al. [15] have shown that the correlation between Doppler and collisional broadening depends on the ratio of perturber and emitter masses $\alpha = m_P/m_E$ and can be neglected only in the case when the emitter mass m_E is much greater than that m_P of the perturber, i.e. for systems with very small values of α. For such systems and in the impact limit when the collision duration is assumed to be negligibly short the resulting line shape can be described by the well-known Voigt profile (VP) which is a convolution of Lorentzian and Gaussian profiles. If, however, for systems with small α-values the finite duration of collision is taken into account then in the first approximation the line shape can be described by the asymmetric Voigt profile (AVP), i.e. a convolution of the Gaussian profile with a profile represented by the sum of the Lorentzian and dispersion profiles [2, 14, 16].

On the other hand, for systems consisting of heavy perturbers and light emitters collision correlation effects become increasingly apparent with increasing value of α. To include these effects in the impact limit the Lorentzian profile with speed-dependent width (FWHM) $\gamma_L(v_E)$ and shift $\Delta(v_E)$ must be averaged correctly over emitter velocities (v_E) using the Maxwellian distribution. Following Berman [14] such velocity-averaged impact profile will be referred to as the speed-dependent Voigt profile (SDVP). Beyond the impact limit the dispersion-shaped correction to the Lorentzian component should be taken into account which must similarly be averaged over velocities and following Harris et al. [16] profiles obtained in such a way will be referred to as the speed-dependent asymmetric Voigt profiles (SDAVP). In this case apart from the collision-time asymmetry mentioned above another cause of line shape asymmetry occurs due to the correlation between contributions to the intensity distribution coming from the thermal motion and collisions.

In our systematic study [17–20] of collisional effects on the ^{114}Cd 326.1 nm ($5\,^1S_0$–$5\,^3P_1$) intercombination line perturbed by noble gases performed by means of laser-induced fluorescence (LIF) technique, particular attention was paid in order to distinguish between these two effects which both can lead to asymmetry of the profile. The choice of the ^{114}Cd isotope enabled us to avoid the hyperfine and isotopic structure of the Cd 326.1 nm line as well as to neglect line mixing effects. For the Cd–noble gas systems the ratio of perturber and emitter masses α changes between 0.035 for Cd–He and 1.15 for Cd–Xe which made possible the overall study of correlation effects. A good signal-to-noise ratio and negligible instrumental profile enabled us to fit the line shapes in considerable detail and record deviations

from the ordinary Voigt profile. In the case of the Cd–Xe ($\alpha = 1.15$) and Cd–Kr ($\alpha = 0.74$) systems we found both the asymmetry of the 326.1 nm line shape caused by collision time asymmetry and that due to correlation between Doppler and collisional broadening. In the case of perturbation by argon ($\alpha = 0.35$), neon ($\alpha = 0.18$), and helium ($\alpha = 0.035$) the influence of the correlation effect on the resulting line shape was not observed.

The values of collision-time asymmetry coefficients determined in Refs. [17–20] were interpreted in the framework of Anderson and Talman [3] and Szudy and Baylis [5, 6] theories. It should be emphasized that these two treatments are fully adiabatic in nature so that they ignore coupling between different molecular states and thus ignore non-adiabatic effects caused by collision-induced transitions between these states. Such non-adiabatic processes are usually very important in the near-wing region where the collision-time asymmetry may appear [10, 11].

In our earlier paper [13] we have developed a semiclassical method which permits the inclusion of the non-adiabatic effects in calculations of both the collision-time asymmetry coefficient and the pressure broadening and shift coefficients. Any calculations of these coefficients require the use of potential curves describing the interaction between the radiating and perturbing atoms. For Cd–noble gas systems such potential curves were first calculated by Czuchaj and Stoll [21] within a pseudopotential self-consistent field/configuration interaction method (SCF/CI). One of us [22] has recently performed tests of the quality of these potential curves by comparing results of his calculations of the pressure broadening and shift coefficients of the ^{114}Cd 326.1 nm line perturbed by noble gases based on the close-coupling (CC) method. The general conclusion drawn in paper [22] was that the CC pressure broadening and shift coefficients are in fairly good agreement with experimental data (except the shift for Cd–He). The calculations performed in paper [22] were done in the framework of the quantum-mechanical impact approximation so that the collision-time asymmetry has not been considered. The main purpose of the present paper is to calculate the collision-time asymmetry coefficient for the ^{114}Cd 326.1 nm line perturbed by noble gases using the semiclassical method developed by Ciuryło et al. [13]. In our present calculation we have used like in paper [22] the potential curves calculated by Czuchaj and Stoll [21] as well as a new version of potential curves for Cd–noble gas atom systems reported recently by Czuchaj et al. [23]. Since these new potential curves were not employed in [22] in the present paper we also report results of the new CC calculations of the pressure broadening and shift coefficients based on new results of Czuchaj et al. [23].

2. Line shape parameters

The collisional component of the line profile $I_C(\widetilde{\nu})$ can be presented as a sum of the Lorentzian and dispersion profiles [2, 5]:

$$I_{\mathrm{C}}(\widetilde{\nu}) = I_{\mathrm{C}}^{(0)}\left(\frac{\gamma_{\mathrm{L}}}{2}\right)\frac{\gamma_{\mathrm{L}}/2 + \chi(\widetilde{\nu}-\widetilde{\nu}_0-\Delta)}{(\widetilde{\nu}-\widetilde{\nu}_0-\Delta)^2+(\gamma_{\mathrm{L}}/2)^2}. \tag{1}$$

Here γ_{L}, Δ, and χ denote the Lorentzian width (FWHM), pressure shift, and collision-time asymmetry parameter, respectively, $I_{\mathrm{C}}^{(0)}$ is the intensity in the line peak and $\widetilde{\nu}_0$ is the unperturbed wave number of the emitted line.

The Lorentzian width Γ_{L} and shift Δ can be evaluated from the following expression [1, 11, 12]:

$$\frac{\gamma_{\mathrm{L}}}{2} + \mathrm{i}\Delta = \frac{N}{c}\int \mathrm{d}^3\boldsymbol{v} f(\boldsymbol{v}) v \int_0^{+\infty} \mathrm{d}\rho\rho \left\{1 - \left\langle S_{\mathrm{ii}}(\rho, v) S_{\mathrm{ff}}^{-1}(\rho, v)\right\rangle_{\mathrm{Ang.Av.}}\right\}. \tag{2}$$

Here N is the perturber density, ρ is the impact parameter, $f(\boldsymbol{v})$ is the Maxwellian distribution of the relative velocities $\boldsymbol{v}$ of the colliding atoms and $S_{\mathrm{ii}}(\rho, v)$ and $S_{\mathrm{ff}}(\rho, v)$ are the matrix elements of the scattering operator $\widehat{S} = \widehat{U}(-\infty, +\infty)$ for the initial and final states of the radiating atom expressed as functions of ρ and v. Here $\widehat{U}(t_2, t_1)$ denotes the time evolution operator and the symbol $\langle \ldots \rangle_{\mathrm{Ang.Av.}}$ means the average over angular coordinates. The collision-time asymmetry parameter can be evaluated from the expression derived in Ref. [13]:

$$\begin{aligned}\chi = 2\pi N \int \mathrm{d}^3\boldsymbol{v} f(\boldsymbol{v}) v \int_0^{+\infty} \mathrm{d}\rho\rho \int_{-\infty}^{+\infty} \mathrm{d}t_0 \\ \times \mathrm{Im}\Big\{1 + \Big\langle U_{\mathrm{ii}}(+\infty, -\infty) U_{\mathrm{ff}}^{-1}(+\infty, -\infty) - U_{\mathrm{ii}}(t_0, -\infty) U_{\mathrm{ff}}^{-1}(t_0, -\infty) \\ - U_{\mathrm{ii}}(+\infty, t_0) U_{\mathrm{ff}}^{-1}(+\infty, t_0)\Big\rangle_{\mathrm{Ang.Av.}}\Big\}.\end{aligned} \tag{3}$$

The angular average $\{U_{\mathrm{ii}}(t_2, t_1) U_{\mathrm{ff}}^{-1}(t_2, t_1)\}_{\mathrm{Ang.Av.}}$ is given by the following equation [24, 25]:

$$\begin{aligned}\{U_{\mathrm{ii}}(t_2, t_1) U_{\mathrm{ff}}^{-1}(t_2, t_1)\}_{\mathrm{Ang.Av.}} = \sum_{m_{\mathrm{i}}, m_{\mathrm{f}}, m_{\mathrm{i}}', m_{\mathrm{f}}', M} (-1)^{2j_{\mathrm{i}} + m_{\mathrm{i}} + m_{\mathrm{i}}'} \\ \times \begin{pmatrix} j_{\mathrm{f}} & 1 & j_{\mathrm{i}} \\ m_{\mathrm{f}} & M & -m_{\mathrm{i}} \end{pmatrix} \times \begin{pmatrix} j_{\mathrm{f}} & 1 & j_{\mathrm{i}} \\ m_{\mathrm{f}}' & M & -m_{\mathrm{i}}' \end{pmatrix} \\ \times \langle j_{\mathrm{i}} m_{\mathrm{i}} | \widehat{U}_{\mathrm{ii}}(t_2, t_1) | j_{\mathrm{i}} m_{\mathrm{i}}' \rangle \langle j_{\mathrm{f}} m_{\mathrm{f}} | \widehat{U}_{\mathrm{ff}}^{-1}(t_2, t_1) | j_{\mathrm{f}} m_{\mathrm{f}}' \rangle.\end{aligned} \tag{4}$$

We treat the collision between emitter and perturber semi-classically, using the straight line trajectory approximation. We assume that the emitter is fixed in the origin of the collisional reference frame while the perturber moves on the straight line trajectory with the constant velocity $\boldsymbol{v}$ and impact parameter ρ. The distance R at time t between emitter and perturber is thus given by $R = \sqrt{\rho^2 + v^2 t^2}$.

In order to describe the collision process, we follow Baranger [11] and use two different reference frames:

1) fixed collisional frame $OX_cY_cZ_c$ with the quantization axis OZ_c perpendicular to the collision plane and OY_c axis directed along the impact parameter ρ,

2) molecular frame $OX_mY_mZ_m$, rotating around OZ_c axis, with the quantization axis OZ_m directed along the $\boldsymbol{R}$ vector and OY_m axis directed along OZ_c axis of the collisional frame (see Fig. 1). Such a choice of the OZ_m axis is due to the axial symmetry of the interaction potential $V(R)$.

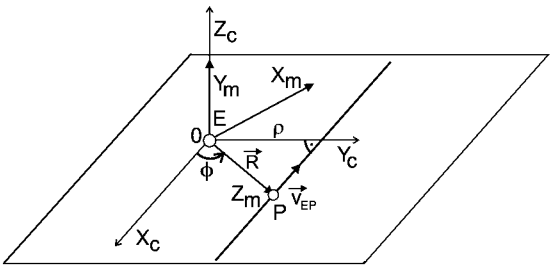

Fig. 1. Two reference frames used to describe the collision process. Details in the text.

The Hamiltonian of the Cd–noble gas system may be written as

$$\widehat{H} = \widehat{H}_0 + \widehat{V}(R), \tag{5}$$

where $\widehat{H}_0 = \widehat{H}_E + \widehat{H}_{SO}$ is the Hamiltonian of the emitter–perturber system for $R \to \infty$ and $\widehat{H}_E$ is the sum of Hamiltonians of the unperturbed Cd and noble gas atoms including electrostatic interaction in the Cd and rare gas (Rg) atoms, H_{SO} is the spin–orbit interaction in the Cd atom.

As the collision is a time-dependent process one should solve the time--dependent Schrödinger equation

$$\mathrm{i}\hbar\frac{\partial|\Psi_k^{(s)}(t)\rangle}{\partial t} = \widehat{H}|\Psi_k^{(s)}(t)\rangle. \tag{6}$$

The state $|\Psi_k^{(s)}(t)\rangle$ in the Schrödinger representation can be related to state in the interaction representation $|\Psi_k^{(i)}(t)\rangle$ by the relation

$$|\Psi_k^{(s)}(t)\rangle = \exp\Big(-\frac{\mathrm{i}\widehat{H}_0 t}{\hbar}\Big)|\Psi_k^{(i)}(t)\rangle. \tag{7}$$

The state in the interaction representation fulfils the following equation:

$$\mathrm{i}\hbar\frac{\partial|\Psi_k^{(i)}(t)\rangle}{\partial t} = \exp\Big(\frac{\mathrm{i}\widehat{H}_0 t}{\hbar}\Big)\widehat{V}\exp\Big(-\frac{\mathrm{i}\widehat{H}_0 t}{\hbar}\Big)|\Psi_k^{(i)}(t)\rangle. \tag{8}$$

Hereafter we use the interaction representation only and for simplicity we omit the upper index (i).

The state vector $|\Psi_k(t)\rangle$ may be expressed as a series

$$|\Psi_k(t)\rangle = \sum_n a_{nk}(t)|n\rangle, \tag{9}$$

with the initial condition $a_{nk}(-\infty) = \delta_{nk}$.

Calculations of the line shape parameters given by formulae (2) and (3) require the values of the matrix elements of the evolution operator $\widehat{U}$ in the interaction representation. These elements can be expressed in terms of $a_{nk}(t)$ coefficients of Eq. (9). The time evolution of the $|\Psi_k(t)\rangle$ state may be described by the formula

$$|\Psi_k(t)\rangle = \widehat{U}(t,-\infty)|\Psi_k(-\infty)\rangle. \tag{10}$$

Comparing Eq. (9) and (10) and using initial conditions we get

$$\sum_n a_{nk}(t)|n\rangle = \widehat{U}(t,-\infty)\sum_n a_{nk}(-\infty)|n\rangle = \widehat{U}(t,-\infty)|k\rangle, \tag{11}$$

and subsequently

$$\sum_n \langle r|n\rangle a_{nk}(t) = \langle r|\widehat{U}(t,-\infty)|k\rangle. \tag{12}$$

Finally, we obtain for the $a_{rk}(t)$ coefficient the following formula:

$$a_{rk}(t) = \langle r|\widehat{U}(t,-\infty)|k\rangle, \tag{13}$$

which represent the relation between $a_{rk}(t)$ and the matrix elements of evolution operator $\widehat{U}$.

From Eqs. (8) and (9) we can obtain the well-known relation

$$\mathrm{i}\hbar\dot{a}_{rk}(t) = \sum_n \langle r|V|n\rangle \exp\left[\frac{\mathrm{i}}{\hbar}(E_r - E_n)t\right] a_{nk}(t), \tag{14}$$

which gives us the values of $a_{rk}(t)$ coefficients and then the required evolution operator $\widehat{U}$ matrix elements needed for the line shape calculations.

In order to adapt the above approach to the analysis of experimental line shapes for the Cd–noble gas systems, the interatomic potentials involving the Cd ground ($5s^2\ {}^1S_0$) and the excited ($5s5p\ {}^3P_1$) states must first be known. The interaction between the ground state atoms Cd($5s^2\ {}^1S_0$) + noble gas atom (${}^1S_0$) is described by a single potential curve corresponding to the $X^1 0^+$ molecular state. During the collision of the Cd atom excited to the $5s5p\ {}^3P_1$ state two molecular states labelled as $A^3 0^+$ and $B^3 1$ are formed which are described by two different potential curves. The broadening and shift of the Cd 326.1 nm intercombination line ($5s5p\ {}^3P_1 - 5s^2\ {}^1S_0$) is thus the result of contributions from the $A^3 0^+ - X^1 0^+$ and $B^3 1 - X^1 0^+$ transitions.

During the collision process the change of the emitter–perturber distance causes the change of electrostatic and spin–orbit interaction as well as rotational energy $\hbar\dot{\phi}$ of the considered quasi-molecule. The relations between the above energies are related with appropriate Hund's cases. Masnou-Seeuws and McCarroll [26] carefully considered validity conditions for different Hund's cases. Following the estimation presented in an earlier paper [27] we can make an assumption that for Cd–noble gas atom collisions Hund's case C is valid throughout the collision.

In this case the interaction matrix V is diagonal in the $|\Omega\rangle$ representation, where Ω is the absolute value of the projection of the total momentum $\boldsymbol{J}$ on the internuclear axis of the Cd–noble gas atom system.

In the calculations of matrix elements of evolution operator U for ^{114}Cd isotope we can neglect non-adiabatic effects due to transition between the levels of the fine structure. It is due to the fact that distances between adjacent levels of the fine structure are relatively large [28]: $W(5\,^3P_1) - W(5\,^3P_0) = 542.113\ \mathrm{cm}^{-1}$ and $W(5\,^3P_1) - W(5\,^3P_2) = -1170.866\ \mathrm{cm}^{-1}$, and that the quenching cross-section of the $5\,^3P_1$ state is very small [29, 30]. Therefore in calculations of the S matrix elements these non-adiabatic effects were omitted. However, we have included the non-adiabatic effects due to the rotation of the molecular axis. In such a case the set of Eqs. (7) leads to four equations. One equation is for the $5\,^1S_0$ state, with the $a'_0(t)$ coefficient, and three equations for the $5\,^3P_1$ state with the $a_{-1}(t)$, $a_0(t)$ and $a_{+1}(t)$ for $m_k = -1, 0, +1$, respectively. The element of the interaction matrix is given by

$$\langle k|V|s\rangle = \langle j_k m_k|V|j_s m_s\rangle = \langle j m_k|V|j m_s\rangle. \tag{15}$$

The interaction matrix (see e.g. [31, 32]) is hermitian and fulfils the following conditions:

$$\langle j_k m_k|V|j_s m_s\rangle = (-1)^{j_s+j_k}\langle j_k\ -m_k|V|j_s\ -m_s\rangle^*, \tag{16}$$

$$\langle j_k m_k|V|j_s m_s\rangle \neq 0 \qquad \text{for} \quad m_k - m_s = 0, \pm 2, \pm 4, \ \ldots \tag{17}$$

The relation between the elements of the interaction matrix V given in collisional $|jm\rangle$ and rotating molecular $|\Omega\rangle$ reference frames is given by elements of the reduced rotation matrix $d^j_{\Omega,m}$ (see e.g. [33]):

$$\begin{aligned}\langle j m_k|V|j m_s\rangle = &\sum_{\Omega}(-1)^{\Omega-m_k}\mathrm{e}^{-\mathrm{i}\phi(m_k-m_s)}\\ &\times d^j_{-\Omega,-m_k}\left(\frac{\pi}{2}\right) d^j_{\Omega,m_s}\left(\frac{\pi}{2}\right)\langle\Omega|V|\Omega\rangle,\end{aligned} \tag{18}$$

where the matrix elements given in the molecular frame $|\Omega\rangle$:

$$\langle\Omega|V|\Omega\rangle = \begin{cases} V_X \text{ for } 5\,^1S_0\ (\Omega = 0), \\ V_A \text{ for } 5\,^3P_1\ (\Omega = 0), \\ V_B \text{ for } 5\,^3P_1\ (\Omega = 1). \end{cases} \tag{19}$$

The non-zero elements of the interaction matrix given in the collisional frame $|jm\rangle$ are

$$\begin{aligned}&\text{for} \quad 5\,^1S_0: \quad \langle 00|V|00\rangle = V_X, \qquad \text{for} \quad 5\,^3P_1: \quad \langle 10|V|10\rangle = V_B,\\ &\langle 11|V|11\rangle = \langle 1\ -1|V|1\ -1\rangle = \tfrac{1}{2}(V_A + V_B) = V_1,\\ &\langle 11|V|1\ -1\rangle = \langle 1\ -1|V|11\rangle^* = \tfrac{1}{2}(V_B - V_A)\mathrm{e}^{-2\mathrm{i}\phi} = f\mathrm{e}^{-2\mathrm{i}\phi}.\end{aligned} \tag{20}$$

Finally the formula (14) leads to the set of the following equations:

$$\mathrm{i}\hbar\dot{a}'_{0,0}(t) = a'_{0,0}(t)V_X, \qquad \mathrm{i}\hbar\dot{a}_{0,0}(t) = a_{0,0}(t)V_B,$$

$$\mathrm{i}\hbar\dot{a}_{-1,m_i}(t) = a_{-1,m_i}(t)V_1 + a_{+1,m_i}(t)f\mathrm{e}^{+2\mathrm{i}\phi},$$
$$\mathrm{i}\hbar\dot{a}_{+1,m_i}(t) = a_{-1,m_i}(t)f\mathrm{e}^{-2\mathrm{i}\phi} + a_{+1,m_i}(t)V_1. \tag{21}$$

It is seen that for $5\,^1S_0$ state we have one equation with $a'_{0,0}(t)$ coefficient and for the $5\,^3P_1$ state we have one separated equation with $a_{0,0}(t)$ coefficient and two sets of two coupled equations with $a_{-1,m_i}(t)$ and $a_{+1,m_i}(t)$ coefficients (where $m_i = -1, +1$). The above set of equations does not have an analytic solution and may be solved only in the numerical way.

It should be noted that calculation of the collisional line width γ_L and shift Δ given by formula (2) requires the values of $\widehat{S} = \widehat{U}(+\infty, -\infty)$ matrix elements, which can be obtained as the asymptotic solution of Eqs. (21) for $t = +\infty$.

Formula (2) can be thus written in a form

$$\frac{\gamma_\mathrm{L}}{2} + \mathrm{i}\Delta = 2\pi N \int \mathrm{d}^3\boldsymbol{v} f_\mu(\boldsymbol{v}) v \int_0^{+\infty} \mathrm{d}\rho\rho$$
$$\times \left[1 - \tfrac{1}{3}(S_{-1,-1} + S_{0,0} + S_{+1,+1}){S'}^{-1}_{0,0}\right]. \tag{22}$$

For the collision-time line asymmetry situation is more complicated. Following the above procedure from Eq. (3) we obtain for the asymmetry factor χ the following formula:

$$\chi = 2\pi N \mathrm{Im} \int \mathrm{d}^3\boldsymbol{v}_{\mathrm{E}Z} f_\mu(\boldsymbol{v}_{\mathrm{E}Z}) v_{\mathrm{E}Z} \int_0^{+\infty} \mathrm{d}\rho\rho$$
$$\times \int_{-\infty}^{+\infty} \mathrm{d}t_0 \Big\{ 1 + \tfrac{1}{3}(S_{-1,-1} + S_{0,0} + S_{+1,+1}){S'_{0,0}}^{-1}$$
$$-\tfrac{1}{3}[U_{-1,-1}(t_0,-\infty) + U_{0,0}(t_0,-\infty) + U_{+1,+1}(t_0,-\infty)]{U'_{0,0}}^{-1}(t_0,-\infty)$$
$$-\tfrac{1}{3}[U_{-1,-1}(+\infty,t_0) + U_{0,0}(+\infty,t_0) + U_{+1,+1}(+\infty,t_0)]{U'_{0,0}}^{-1}(+\infty,t_0)\Big\}. \tag{23}$$

The values of elements of the matrices $U(t_0, -\infty)$, etc. are given in detail in Appendix A.

It is seen that in order to calculate χ we need to know the values of matrix elements for each time t_0 and then to perform integration over t_0. This causes that such calculations are time- and memory-consuming.

2.1. Adiabatic approximation

In the adiabatic approximation we assume that we have one quantization axis directed along the internuclear axis of the Cd–noble gas atom system. It corresponds to the assumption that the only non-zero elements are

$$\langle jm_s|V|jm_s\rangle = \langle\Omega|V|\Omega\rangle.$$

In such a case Eqs. (14) may be written in the form of four non-coupled equations

$$\mathrm{i}\hbar\dot{a}'_{0,0}(t) = a'_{0,0}(t)V_X\,, \qquad \mathrm{i}\hbar\dot{a}_{0,0}(t) = a_{0,0}(t)V_A\,,$$

$$\mathrm{i}\hbar\dot{a}_{-1,-1}(t) = a_{-1,-1}(t)V_B\,, \qquad \mathrm{i}\hbar\dot{a}_{+1,+1}(t) = a_{+1,+1}(t)V_B\,. \tag{24}$$

Thus we have three separated equations for the $^3P_1$ state. Solving them we get the S matrix elements, and from Eq. (2) we get the formulae for the line width γ_{L} and shift Δ:

$$\gamma_{\mathrm{L}} = \tfrac{1}{3}\gamma_{\mathrm{L}(A-X)} + \tfrac{2}{3}\gamma_{\mathrm{L}(B-X)}, \tag{25}$$

$$\Delta = \tfrac{1}{3}\Delta_{(A-X)} + \tfrac{2}{3}\Delta_{(B-X)}. \tag{26}$$

Here $\gamma_{\mathrm{L}(A-X)}$ and $\Delta_{(A-X)}$ denote the line width and shift corresponding to the $A^3 0^+ - X^1 0^+$ (or $B^3 1 - X^1 0^+$) transition in Cd–noble gas atom quasi-molecule which can be written in the form

$$\gamma_{\mathrm{L}(i-X)} = 4N\pi \left\langle v_{\mathrm{E}Z} \int_0^\infty \mathrm{d}\rho\rho[1 - \cos(\eta_{(i-X)})] \right\rangle, \tag{27}$$

$$\Delta_{(i-X)} = 2N\pi \left\langle v_{\mathrm{E}Z} \int_0^\infty \mathrm{d}\rho\rho \sin(\eta_{(i-X)}) \right\rangle, \tag{28}$$

where the index i corresponds either to the $A^3 0^+$ or $B^3 1$ state. It is seen that Eqs. (27) and (28) are identical to the Lindholm–Foley [1] formulae for the $A^3 0^+ - X^1 0^+$ and $B^3 1 - X^1 0^+$ transitions.

The phase shift $\eta_{(i-X)}$ is given by

$$\eta_{(i-X)} = \frac{1}{\hbar} \int_{-\infty}^{\infty} [V_i(t) - V_X(t)]\,\mathrm{d}t. \tag{29}$$

In an analogous way we can obtain the formula for the line asymmetry χ calculated in adiabatic approximation

$$\chi = \tfrac{1}{3}\chi_{(A-X)} + \tfrac{2}{3}\chi_{(B-X)}, \tag{30}$$

where $\chi_{(A-X)}$ and $\chi_{(B-X)}$ are the line asymmetry parameters corresponding to $A^3 0^+ - X^1 0^+$ and $B^3 1 - X^1 0^+$ transitions calculated from Eq. (3).

3. Results and discussion

Using the formulae presented above we have calculated the theoretical values of pressure broadening $\beta = \gamma_{\mathrm{L}}/N$, shift $\delta = \Delta/N$ and asymmetry coefficients $\kappa = \chi/N$ and listed them in Tables I–III, respectively. Our calculations were performed for the Czuchaj and Stoll [21] and Czuchaj et al. [23] potentials both in semiclassical adiabatic (SA) and semiclassical non-adiabatic (SNA) approach including the effects due to the rotation of the molecular axis. In the case of the Czuchaj et al. [23] potential the potential curves were extended (except for Cd–He system) with van der Waals potential. For details see Appendix B. In order to make a comprehensive comparison for the β and δ coefficients in Tables I and II

TABLE I

The values of the pressure broadening β coefficients of the 326.1 nm ^{114}Cd line (in units 10^{-20} cm^{-1}/atom cm^{-3}) calculated in semiclassical adiabatic, semiclassical non-adiabatic and quantum-mechanical close-coupling approach together with experimental values. Numbers in parentheses are the values of standard uncertainty (temperature $T = 724$ K for Xe, Kr, Ar, Ne, and $T = 439$ K for He).

Perturber	Czuchaj and Stoll [21]			Czuchaj et al. [23]			Experimental
	SA	SNA	CC [22]	SA	SNA	CC	
Xe	1.330	1.352	1.466	1.076	1.082	1.183	1.257 (0.006)
Kr	1.182	1.214	1.371	0.996	0.973	0.857	1.147 (0.011)
Ar	1.334	1.347	1.453	0.864	0.854	0.682	1.060 (0.006)
Ne	0.750	0.753	0.806	0.761	0.767	0.879	0.715 (0.004)
He	1.091	1.091	1.263	0.521	0.859	0.995	1.155 (0.034)

TABLE II

The values of the pressure shift δ coefficients (in units 10^{-20} cm^{-1}/atom cm^{-3}) calculated in semiclassical adiabatic, semiclassical non-adiabatic, and quantum--mechanical close-coupling approach together with experimental values. Numbers in parentheses are the values of standard uncertainty (temperature $T = 724$ K for Xe, Kr, Ar, Ne, and $T = 439$ K for He).

Perturber	Czuchaj and Stoll [21]			Czuchaj et al. [23]			Experimental
	SA	SNA	CC [22]	SA	SNA	CC	
Xe	–0.322	–0.328	–0.325	–0.252	–0.266	–0.341	–0.348 (0.002)
Kr	–0.181	–0.195	–0.245	0.189	0.181	–0.032	–0.338 (0.005)
Ar	–0.358	–0.371	–0.499	–0.120	–0.127	–0.123	–0.387 (0.004)
Ne	–0.142	–0.143	–0.071	0.221	0.220	0.220	–0.090 (0.005)
He	0.067	0.067	0.234	–0.313	–0.316	0.109	–0.031 (0.009)

we also included the values resulting from the quantum close-coupling (CC) calculations for the Czuchaj and Stoll [21] potentials presented in paper [22]. Tables I and II also contain results of new CC calculations of β and δ coefficients performed during the course of the present investigation on the basis of new potential curves reported by Czuchaj et al. [23]. For the asymmetry coefficients (κ) the close-coupling calculations are planned in the nearest future. In Tables I–III we also present experimental values of above coefficients determined in previous work in this laboratory [17–20].

As can be seen from Tables I–III the inclusion of the rotation of the atomic axis in the semiclassical treatment does not lead to the improvement of the agreement between calculated and experimental values in comparison to what results from the purely adiabatic calculations.

TABLE III

The values of the asymmetry coefficients κ (in units 10^{-21}/atom cm^{-3}) calculated in semiclassical adiabatic and semiclassical non-adiabatic approach together with experimental values. Numbers in parentheses are the values of standard uncertainty (temperature $T = 724$ K for Xe, Kr, Ar, Ne, and $T = 439$ K for He).

Perturber	Czuchaj and Stoll [21]		Czuchaj et al. [23]		Experimental
	SA	SNA	SA	SNA	
Xe	–1.15	–1.21	–1.07	–1.07	–1.08 (0.07)
Kr	–0.99	–1.06	–0.16	–0.15	–1.00 (0.07)
Ar	–0.85	–0.88	–0.16	–0.14	–0.30 (0.05)
Ne	–0.03	–0.02	0.15	0.15	–0.17 (0.07)
He	0.09	0.10	–0.15	–0.11	0.62 (0.34)

The general conclusion which can be drawn from data listed in Tables I and II is that for Cd–Xe in the quantum close-coupling treatment the new potential curves of Czuchaj et al. [23] reproduce better the experimental data of β and δ than those employing the Czuchaj and Stoll [21] potentials. Contrary to that in the semiclassical approach the Czuchaj and Stoll [21] potentials seem to give better agreement. As it is seen from Table III the asymmetry parameter for Cd–Xe calculated semiclassically on the basis of these new potentials yields values which are in better agreement with experiment than those based on the potentials reported by Czuchaj and Stoll [21]. On the other hand, however, for Cd–Kr, Cd–Ar, and Cd–Ne the Czuchaj–Stoll potentials seem to reproduce the experimental data much better than the new potentials by Czuchaj et al. [23]. For Cd–He reasonable agreement is obtained only for the broadening coefficient both in the semiclassical and quantum CC case.

Acknowledgment

The authors wish to express their gratitude to Professor J. Szudy for valuable help in the preparation of the manuscript and to Professor E. Czuchaj for making available the values of numerical potentials.

This work was supported by a grant No. 5 PO3B 066 20 (354/PO3/2001/20) from the State Committee for Scientific Research.

Appendix A

The explicit values of the matrix elements appearing in Eqs. (22) and (23) represented in terms of expansion coefficients $a_{rk}(t)$ are given by the formulae

$$S_{m_i,m_i} = U_{m_i,m_i}(+\infty,-\infty) = a_{m_i,m_i}(+\infty), \tag{A1}$$

$$U_{m_i,m_i}(t,-\infty) = a_{m_i,m_i}(t), \tag{A2}$$

$$U_{0,0}(+\infty,t) = a_{0,0}(+\infty)a_{0,0}^{-1}(t). \tag{A3}$$

Using relation $\widehat{U}(+\infty,t) = \widehat{U}(+\infty,-\infty)\widehat{U}^{-1}(t,-\infty)$ one can show that

$$U_{-1,-1}(+\infty,t) = \left[a_{-1,-1}(+\infty)a_{-1,-1}^{-1}(t) - \frac{a_{-1,+1}(+\infty)a_{+1,-1}(t)}{a_{+1,+1}(t)a_{-1,-1}(t)}\right] \times \left[1 - \frac{a_{+1,-1}(t)a_{-1,+1}(t)}{a_{+1,+1}(t)a_{-1,-1}(t)}\right]^{-1}, \tag{A4}$$

$$U_{+1,+1}(+\infty,t) = \left[a_{+1,+1}(+\infty)a_{+1,+1}^{-1}(t) - \frac{a_{+1,-1}(+\infty)a_{-1,+1}(t)}{a_{+1,+1}(t)a_{-1,-1}(t)}\right] \times \left[1 - \frac{a_{+1,-1}(t)a_{-1,+1}(t)}{a_{+1,+1}(t)a_{-1,-1}(t)}\right]^{-1}. \tag{A5}$$

It should be noted that in some cases we can use an approximate formulae for $U_{-1,-1}(+\infty,t)$ and $U_{+1,+1}(+\infty,t)$ matrix elements [33]. If we neglect the off-diagonal a_{m_i,m_j} elements the two above equations can be presented in a form similar to Eq. (A3): $U_{-1,-1}(+\infty,t) = a_{-1,-1}(+\infty)a_{-1,-1}^{-1}(t)$ and $U_{+1,+1}(+\infty,t) = a_{+1,+1}(+\infty)a_{+1,+1}^{-1}(t)$. Such approach in line asymmetry calculations is less time- and memory-consuming but on the other hand is of less accuracy.

Appendix B

The line shape parameters γ, Δ, and χ are in principle dependent on the values of the interaction potentials in the entire region of interaction distances R. Only for the inverse-power $V(R) = -C_q R^{-q}$ potentials these parameters can be evaluated analytically. For other (more realistic) interaction potentials numerical methods must be used.

For numerical potentials there are two crucial points. The values of the interaction potentials should be tabulated in wide range of interatomic distances R, with relatively low increment of R (which is unfortunately time-consuming). The accuracy of calculations resulting from the applied potential model and numerical aspects should be high enough, especially for the large R-values.

In order to justify the above requirements we performed appropriate numerical tests described in detail in [34]. We found that the difference of the interaction potentials in the initial (i) and final (f) states $\Delta V(R) = V_{\rm i}(R) - V_{\rm f}(R)$ (like in Eq. (29)) should be known with accuracy not worse than 0.01 cm^{-1}. This means that a single potential curve should be calculated with 0.005 cm^{-1} accuracy. For the line shift calculation a crucial role is played by the accuracy of potential values in the range of large R-values. It was shown [34] that for the line shift the contribution coming from R larger than 20 a.u. may exceed 20% of its total value.

If the interaction potentials do not meet these requirements calculations of the line shape parameters may lead to entirely wrong results. Such problems occur for Cd–rare gas potentials calculated recently by Czuchaj et al. [23]. As an example in Table IV we present the values of their last tabulated points of the $B^3 1$ Cd–Ar potential curve. As it can be seen the last non-zero value equal to –0.4 cm^{-1} occurs for $R = 25$ a.u. and the next point is the zero value for $R = 50$ a.u. Thus the following question arises: What are the values of the interaction potential located between the value –0.4 cm^{-1} for $R = 25$ a.u. as calculated by Czuchaj et al. [23] and its asymptotic zero value assumed for $R = 50$ a.u. To answer this question we considered four cases.

TABLE IV

The values of the $B^3 1$ Cd–Ar [23] potential curve for $R \geq 20$ a.u.

R [a.u.]	$V(R)$ [cm^{-1}]
...	...
20.0	–1.0
21.0	–0.8
22.0	–0.6
23.0	–0.5
24.0	–0.4
25.0	–0.4
50.0	0.0

Case I: For $R < 25$ a.u. we used the values $A^3 0^+$, $B^3 1$, and $X^1 0^+$ potential curves calculated by Czuchaj et al. [23]. For 25 a.u. $< R <$ 50 a.u. the interaction potentials were interpolated using a parabolic interpolation.

Case II: For $R < 25$ a.u. we used as in case I the values computed by Czuchaj et al. [23] but for $R > 25$ a.u. we extended the potential curves assuming the van der Waals form $V(R) = -C_6 R^{-6}$ with C_6 constants determined by fitting to the Czuchaj et al. [23] potential at the last non-zero point, i.e. at $R = 25$ a.u.

Case III: We extended the Czuchaj et al. [23] potential with van der Waals potential starting from $R = 21$ a.u.

Finally, in **Case IV** we extended the potential curves performing least squares fitting of the van der Waals potential to the six last non-zero points on each curve.

In Table V we have listed the values of β, δ, and κ coefficients calculated in cases I–IV. It is seen that the values of the β coefficient calculated for three (II–IV) different ways of extending the potential curves with the van der Waals potential are close to each other but the values of the shift coefficient δ differ more significantly. It is seen that there is no unambiguous criterion which way of extension is proper and guarantee reliable results of β, δ, and κ coefficients calculations. It seems that the requirement concerning the $\Delta V(R) < 0.01$ cm^{-1} accuracy cannot

be fulfilled now due to the limitations of the physical model applied in the potential calculations as well as computational abilities (memory- and time-consuming). It should be also noted that for larger interatomic R distances the calculated values of potentials may be at random and the required accuracy is not sure.

TABLE V

The comparison of pressure broadening β, shift δ, and asymmetry κ coefficients calculated for Cd–Ar system using Czuchaj et al. [23] potential curves assuming "different ways" of reaching the asymptotic zero value.

Case	β	δ	κ
I	2.538	–2.351	–3.89
II	0.884	–0.342	–0.29
III	0.854	–0.097	–0.14
IV	0.857	–0.155	–0.16

TABLE VI

The values of C_6 force constants of the van der Waals extension potentials (in units 10^7 cm$^{-1}[a_0]^6$) obtained from the fitting procedure. $R_{\rm con}$ — connection point.

	$X^1 0^+$	$A^3 0^+$	$B^3 1$	$R_{\rm con}$ [a.u.]
Cd–Ne	2.23	0.78	1.90	22
Cd–Ar	5.50	4.23	6.82	22
Cd–Kr	1.26	6.17	9.35	27
Cd–Xe	14.4	18.6	16.0	28

Taking all the above into account in both adiabatic and non-adiabatic calculations of the β, δ, and κ coefficients for Czuchaj et al. [23] potentials we decided to perform the potential curves extension by fitting the van der Waals potential to the six last non-zero points on each curve. The original potential curve and the van der Waals potential curve were then connected in the point $R_{\rm con}$ of their closest approach. This procedure was not necessary in the case of the Cd–He system where for all potential curves there was not a large gap between last non-zero point and appropriate zero point. In Table VI we present the values of C_6 force constants of the van der Waals extension potentials obtained from the least squares best-fit procedure, together with the values of connection points $R_{\rm con}$.

References

[1] N. Allard, J. Kielkopf, *Rev. Mod. Phys.* **54,** 1103 (1982).

[2] J. Szudy, W.E. Baylis, *Phys. Rep.* **266,** 127 (1996).

[3] P.W. Anderson, J.D. Talman, Bell Teleph. Syst. Tech. Publ. No. 3117, University of Pittsburg, USA, 1955.

[4] G. Traving, *Über die Theorie der Druckverbreiterung von Spektrallinien*, Verlag G. Braun, Karlsruhe 1960.

[5] J. Szudy, W.E. Baylis, *J. Quant. Spectrosc. Radiat. Transf.* **15,** 641 (1975).

[6] J. Szudy, W.E. Baylis, *J. Quant. Spectrosc. Radiat. Transf.* **17,** 681 (1977).

[7] G. Peach, *J. Phys. B* **17,** 2599 (1984).

[8] B.N.I. Al-Saqabi, G. Peach, *J. Phys. B* **20,** 1175 (1987).

[9] A. Royer, *Acta Phys. Pol. A* **54,** 805 (1978).

[10] P.S. Julienne, F.H. Mies, *Phys. Rev. A* **34,** 3792 (1986).

[11] M. Baranger, *Phys. Rev.* **111,** 494 (1958); *Phys. Rev.* **112,** 855 (1958).

[12] R. Ciuryło, *Phys. Rev. A* **58,** 1029 (1998).

[13] R. Ciuryło, J. Szudy, R.S. Trawiński, *J. Quant. Spectrosc. Radiat. Transf.* **57,** 551 (1997).

[14] P.R. Berman, *J. Quant. Spectrosc. Radiat. Transf.* **12,** 1331 (1972).

[15] J. Ward, J. Cooper, E.W. Smith, *J. Quant. Spectrosc. Radiat. Transf.* **14,** 555 (1974).

[16] M. Harris, E.L. Lewis, D. McHugh, I. Shannon, *J. Phys. B* **17,** L661 (1984).

[17] A. Bielski, R. Ciuryło, J. Domysławska, D. Lisak, R.S. Trawiński, J. Szudy, *Phys. Rev. A* **62,** 032511 (2000).

[18] R.S. Trawiński, A. Bielski, D. Lisak, *Acta Phys. Pol. A* **99,** 243 (2001).

[19] A. Bielski, D. Lisak, R.S. Trawiński, *Eur. Phys. J. D* **14,** 27 (2001).

[20] A. Bielski, D. Lisak, R.S. Trawiński, J. Szudy, *Acta Phys. Pol. A* **103,** 23 (2003).

[21] E. Czuchaj, H. Stoll, *Chem. Phys.* **248,** 1 (1999).

[22] T. Orlikowski, *Eur. Phys. J. D*, 2003, in press.

[23] E. Czuchaj, M. Krośnicki, H. Stoll, *Theor. Chem. Acc.* **105,** 219 (2001).

[24] C.S. Tsao, R. Curnutte, *J. Quant. Spectrosc. Radiat. Transf.* **2,** 41 (1962).

[25] J. Cooper, *Rev. Mod. Phys.* **39,** 167 (1967).

[26] F. Masnou-Seeuws, R. McCarroll, *J. Phys. B, At. Mol. Phys.* **7,** 2230 (1974).

[27] A. Bielski, S. Brym, R. Ciuryło, J. Domysławska, R.S. Trawiński, M.G. Lednev, *Acta Phys. Pol. A* **90,** 1155 (1997).

[28] C.E. Moore, *Atomic Energy Levels*, NSRDS-NBS, Vol. 3, U.S. Dep. of Commerce, National Bureau of Standards, Washington 1971.

[29] M. Czajkowski, E. Walentynowicz, L. Krause, *J. Quant. Spectrosc. Radiat. Transf.* **28,** 13 (1982).

[30] H. Umemoto, T. Ohnuma, A. Masaki, *Chem. Phys. Lett.* **4,** 357 (1990).

[31] E.J. Roueff, *J. Phys. B, At. Mol. Phys.* **7,** 185 (1974).

[32] D.F.T. Mullamphy, G. Peach, I.B. Whittingham, *J. Phys. B, At. Mol. Opt. Phys.* **24,** 3709 (1991).

[33] D.M. Brink, G.R. Satchler, *Angular Momentum*, Oxford University Press, Oxford 1971.

[34] R.S. Trawiński, *Asymmetry of 326.1 nm Cadmium Spectral Line Perturbed by Noble Gases*, Wydawnictwo Uniwersytetu Mikołaja Kopernika, Toruń 2002 (in Polish).